Atmos. Chem. Phys. Discuss., 10, 2221–2244, 2010
www.atmos-chem-phys-discuss.net/10/2221/2010/

Atmospheric Chemistry and Physics Discussions

This discussion paper is/has been under review for the journal Atmospheric Chemistry and Physics (ACP). Please refer to the corresponding final paper in ACP if available.

A trajectory analysis of atmospheric transport of black carbon aerosols to Canadian High Arctic in winter and spring (1990–2005)

L. Huang[1], S. L. Gong[2], S. Sharma[3], D. Lavoué[2], and C. Q. Jia[1]

[1]Department of Chemical Engineering and Applied Chemistry, University of Toronto, 200 College Street, Toronto, ON M5S 3E5 Canada
[2]Air Quality Research Division, Environment Canada, Toronto, ON M3H 5T4 Canada
[3]Climate Research Division, Environment Canada, Toronto, ON M3H 5T4 Canada

Received: 22 October 2009 – Accepted: 13 January 2010 – Published: 1 February 2010

Correspondence to: S. L. Gong (sunling.gong@ec.gc.ca)

Published by Copernicus Publications on behalf of the European Geosciences Union.

Abstract

Black carbon (BC) particles accumulated in the Arctic troposphere and deposited over snow have significant effects on radiative forcing of the Arctic regional climate. Applying cluster analysis technique on 10-day backward trajectories, transport pathways affecting Alert (82.5° N, 62.5° W), Nunavut in Canada are identified in this work, along with the associated transport frequency. Based on the atmospheric transport frequency and the estimated BC emission intensity from surrounding regions, a linear regression model is constructed to investigate the inter-annual variations of BC observed at Alert in January and April, representative of winter and spring respectively, between 1990 and 2005. Strong correlations are found between BC concentrations predicted with the regression model and measured at Alert for both seasons (R^2 equals 0.77 and 0.81 for winter and spring, respectively). Results imply that atmospheric transport and BC emission are the major contributors to the inter-annual variations in BC concentrations observed at Alert in the cold seasons for the 16-year period. Based on the regression model the relative contributions of regional BC emissions affecting Alert are attributed to the Eurasian sector, composed of the European Union and the former USSR, and the North American sector. Considering both seasons, the model suggests that Eurasia is the major contributor to the near-surface BC levels at the Canadian High Arctic site with an average contribution of over 85% during the 16-year period. In winter, the atmospheric transport of BC aerosols from Eurasia is found to be even more predominant with a multi-year average of 94%. The model estimates smaller contribution from the Eurasian sector in spring (70%) than that in winter. It is also found that the change in Eurasian contributions depends mainly on the reduction of emission intensity, while the changes in both emission and atmospheric transport contributed to the inter-annual variation of North American contributions.

ACPD

10, 2221–2244, 2010

1 Introduction

Black carbon (BC) particles accumulated in the Arctic troposphere and deposited onto snow have significant effects on radiative forcing of the Arctic regional and the global climate (Flanner et al., 2007; Hansen and Nazarenko, 2004; Jacobson, 2001; Kristjansson et al., 2005). Absorbing both the direct and the reflected solar radiation, BC in the atmosphere was suggested to be the second strongest contributor to current global warming, after carbon dioxide (Chung et al., 2005; Ramanathan and Carmichael, 2008). Once deposited onto snow and sea ice, BC changes the surface albedo and contributes to melting of Arctic sea ice (Clarke and Noone, 1985; Flanner et al., 2007; Jacobson, 2004; Kim et al., 2005; Koch and Hansen, 2005). BC particles (along with sulphate and organic carbon) intensively accumulate in the Arctic troposphere during the winter and early spring, as a result of the Arctic haze phenomenon (Barrie, 1986; Law and Stohl, 2007; Quinn et al., 2007; Shaw, 1995). The anthropogenic emissions from Europe and former USSR were suggested to be the major sources of the Arctic haze in general (Quinn et al., 2007; Shindell et al., 2008; Stohl, 2006), but the relative importance of the potential source regions may have different impacts on two different sites in the Arctic (Sharma et al., 2006). Worthy et al. (1994), for instance, showed that rapid air mass transport from western Russia in winter was responsible for the highest concentrations of BC measured at Alert.

Based on 13-year continuous observations at Alert (82.5° N, 62.5° W), Nunavut, Canada since 1989, a broad peak in BC concentration was previously found from January to April (Sharma et al., 2006), corresponding to the haze season. Recently, a marked monotonic decreasing trend of BC concentration at Alert between 1989 and 2002 was revealed using a geometric time variation model (Sharma et al., 2004). The impact of emission variation was highlighted in their study as the decreasing trend in BC concentrations was associated to the reduction of BC emissions from the former USSR sector, rather than the North American and the European sectors. Additionally, the important influence of atmospheric transport variability on the inter-annual changes

ACPD
10, 2221–2244, 2010

of air pollution levels in the Arctic troposphere was also revealed recently, particularly the effect of North Atlantic Oscillation (NAO) (Eckhardt et al., 2003). However, studies emphasizing the simultaneous effects of varying atmospheric transport and BC emissions are still limited. More recently, the inter-annual variation of BC was correlated with two atmospheric transport indices derived from the 700 hPa geopotential heights and regional BC emissions, but only 36 and 54% of the variations can be explained for January and April data (Gong et al., 2010). In this paper, an attempt is made to investigate the effect of changes in both emission and atmospheric transport on the inter-annual variation of BC observed at Alert from 1990 through 2005, and to further quantify the contributions of BC emissions from two sectors based on trajectory analysis technique. To better isolate the effect of atmospheric transport in the cold seasons, 10-day backward trajectories in January and April between 1990 and 2005 are used in this study. Transport in January and April are specifically investigated in this study because the atmospheric transport to the Arctic remain strong in these months according to the average length of the 10-day back trajectories arriving at Alert. Applying the cluster analysis technique, the transport pathways affecting Alert are identified for both seasons. Based on the obtained transport frequency from cluster analysis and the estimated BC emission intensity from surrounding regions, a linear regression model is constructed to reconstruct the year-to-year changes in BC surface concentrations in winter and spring.

2 Data and methods

2.1 Equivalent black carbon data

Continuous hourly measurements of the BC at Alert have been conducted since 1989. The attenuation of light transmitted through particles collected on a quartz fiber filter was measured using a commercial aethalometer, along with the attenuation of a blank filter. Then the hourly BC concentrations were calculated based on the difference in

attenuation, the filter area, the sample flow rate, and a specific attenuation coefficient (19 m^2/g). The later is determined based upon calibrations during instrument development and theoretical calculations. More detailed description of the method and the determination of the specific attenuation coefficient were documented by Sharma et al. (2004).

2.2 Trajectory data and transport frequency

Ten-day backward trajectories arriving at 500 m above ground level (or a.g.l.) at Alert were initialized 12 times daily (i.e., 00:00, 02:00, 04:00, ... and 22:00 coordinated universal time) for January and April between 1990 and 2005 using the HYSPLIT model (HYbrid Single-Particle Lagrangian Integrated Trajectory, version 4) (Lin et al., 2001). Three-dimensional wind fields from NCEP/NCAR global reanalysis data (Kalnay et al., 1996) were used to drive HYSPLIT, which are available every 6 h on a 2.5 degree latitude-longitude global grid with 18 vertical levels. The arrival elevation of 500 m a.g.l. locates within the wintertime Arctic inversion layer so that it is representative of the air sampled at Alert. Worthy et al. (1994), for instance, compared trajectories arriving 1000, 925, 850, and 700 hPa above Alert and suggested that the 925 hPa level (about 540 m a.g.l.) was the most representative arriving height. Ten-day backward trajectories are used in this study since trajectories of a shorter duration are usually not long enough to indicate possible distant source regions affecting the Arctic (Harris and Kahl, 1990). Although longer trajectories are generally subject to higher uncertainty, progressive advances in generating meteorological fields, computing trajectories, and especially, the implementation of cluster analysis technique on a large set of trajectories in this study may, to some extent, reduce the effects of individual errors (Harris and Kahl, 1994; Kahl, 1990). The clustering algorithm described by Dorling et al. (1992) was modified (refer to Supporting Information: Modified Dorling's algorithm, http://www.atmos-chem-phys-discuss.net/10/2221/2010/acpd-10-2221-2010-supplement.pdf) to effectively group trajectories. Each group of trajectories represents a distinct transport pathway bringing air masses into Alert. The

transport frequency (dimensionless) for every pathway can be estimated by computing the percentage of trajectories in that group.

2.3 Surface flux of BC

Wintertime black carbon emissions in the northern mid-latitudes are predominantly emitted from incomplete fossil fuel combustion. Analyzing BC trend in the Arctic required building annual BC emission inventories by country from 1990 through 2005. BC emissions were calculated globally from consumption and transaction amounts of 23 different fuel types compiled by the United Nations (United Nations, 2007). The method to compute emissions was initially developed by (Cooke et al., 1999) for 1970–1989. The period was extended a first time to 1990–1998 in (Sharma et al., 2004) and through 2005 in (Sharma et al., 2009). BC emissions located in the former USSR decreased by more than 50% during the first half of the 1990s, and since then have progressively increased. In addition, South Asian emissions steadily increased during the 1990s and have accelerated since the early 2000s, reaching +10% per year. Global emissions were also developed by (Bond et al., 2007). Only emissions every 10 years until 2000 are made available to the public on their web site (http://www.hiwater.org). For the year 2000, we determined global emissions of 7200 Gg, while they totalized 4537 Gg, i.e. 37% less. For 1990, the difference calculated is similar.

Based on the previous study on the atmospheric transport into the Arctic troposphere (Stohl, 2006), North America (50–180° W), European Union (15° W–15° E) and the former USSR (15–180° E) are considered as the major BC source regions affecting Alert through the lower troposphere transport in this work. The obtained BC surface fluxes from these regions for 1990–2005 are shown in Fig. 1. A pronounced decreasing trend in BC surface flux is found for the former USSR sector while the emissions from the European Union and the North American sectors increase stably during the same period.

2.4 Simple linear regression model

A mass balance approach is used to establish the linkage among the intensity of anthropogenic emission, the frequency of atmospheric transport, and the measured BC, which has the following formula

$$[\mathrm{BC}]_{\mathrm{Jan/Apr},j} = \sum_{i=1}^{n} (f_{i,j} \cdot C_{i,j}) \quad (1)$$

where $i = 1, 2, \ldots, n$ is an arbitrary index for atmospheric transport pathways affecting Alert and $j = 1990, 1991, \ldots, 2005$ represents year from 1990 through 2005. For the year of j, the left-hand side of the above equation represents the monthly average BC concentration observed in January or April (in ng/m^3), $f_{i,j}$ (in percentage) is the transport frequency of the i-th pathway, and $C_{i,j}$ (in ng/m^3) is defined as the BC concentration that would be measured if only the i-th transport pathway had affected the receptor.

It is then assumed in this study that the characteristic BC concentration of a transport pathway is linearly proportional to the surface flux of BC emission at source region identified by trajectory cluster analysis. The mass balance model takes the following form,

$$[\mathrm{BC}]_{\mathrm{Jan/Apr},j} = \sum_{i=1}^{n} (f_{i,j} \cdot b_i \cdot E_{i,j}) \quad (2)$$

where $E_{i,j}$ (in ng/m^2/s) represents the surface flux of BC emission from source region i in the year of j and b_i (in s/m) is a cluster specific proportional constant. The final form of the mass balance model shows a linear dependence of monthly average BC concentration ([BC]) on transport frequency (**f**) and emission intensity (**E**), which are obtained following the methodologies described in Sect. 2.1–2.3. It is a simple linear regression model with the independent variable or predictor $\sum_{i=1}^{n} (f_{i,j} \cdot E_{i,j})$ and the slope

ACPD
10, 2221–2244, 2010

b_i. It is physically meaningful to have a zero intercept in this model, which requires that other BC emissions than those considered in this study have little impact on the near-surface BC observed at Alert. Using a particle dispersion model, the BC source contribution to the entire Arctic troposphere from south Asia was estimated to be only 10% of the European value (Stohl, 2006). The number would be even smaller for the case of high Arctic surface, such as the underlying receptor, Alert. Given BC concentrations, transport frequencies, and emission intensities, the slope (b_i) is estimated using the least squares method. The purpose of introducing the **b** factors is to relate the available surface emission inventories to the observed concentrations at the receptor when atmospheric transport from source regions takes place. The **b** factors are assumed to be the ratio of the concentration in the air to the surface emission flux. So it is region specific and it has the unit of s/m. It may depend on factors, such as the horizontal wind speed, precipitation, and air mass mixing during the transport.

3 Results and discussion

3.1 Transport pathways affecting Alert

Ten-day backward trajectories for January and April from 1990 through 2005 are classified into 7 distinct groups by implementing the modified clustering algorithm. The cluster-mean trajectories, which indicate the average atmospheric flow patterns, are shown in Fig. 2. The identified 7 transport pathways are distinct in wind direction and speed. First of all, there are several specific characteristics that can be found for the air masses arriving at Alert in January. In terms of wind direction, it was found that southerly (clusters 1, 2, and 3) and northerly (clusters 4, 5, 6, and 7) flows dominate the wintertime atmospheric transport. For the period of interest, northerly winds constitute slightly over 50% of the total flows and the rest is from southerly transport. Among southerly transport routes, clusters 2 and 3 indicate transport of air masses from south and southwest to the receptor Alert. Cluster 2 appears to be the most frequent trans-

ACPD
10, 2221–2244, 2010

port pathway, which alone accounts for 20% of the air masses affecting Alert. The cluster-member plot for cluster 2 (not shown in this paper) indicates that most of the trajectories in this group originally started from Canada or Alaska, moved first towards southeast of Canada, and turned north between Baffin Island and Greenland due to the effect of geographic barrier. Cluster 3 (about 11%) is composed of trajectories with a strong westerly wind component. The trajectories in this cluster are mostly found to originate between Eastern Siberia and the Beaufort Sea, although few are found from Bering Sea. Cluster 1 (17%), however, contains trajectories passing through the European Arctic region. Trajectories in this cluster initiated from the North Atlantic Ocean and the Europe.

Among the northerly transport pathways in Fig. 2a, cluster 5 is characterized as a relatively slow northerly moving group, which is found about 14% of the time in January. Trajectories grouped into this cluster initiated from the northern high latitudes of the former USSR, but they are found cycling around the Alert site. During the 10-day transport to Alert, trajectories in this group spent considerable amount of time in traveling above the sea ice covering the Arctic Ocean. In January, several fully developed long-range transport pathways bringing air masses from Eurasia into Alert are found with considerable frequency of occurrence. This type of pathways includes clusters 4, 6, and 7 in Fig. 2a. Cluster 7 (about 10%) represents the transport of mid-latitude continental air masses from Eastern Europe. A number of trajectories in this cluster extend deeply into the mid-latitudes as far south as 45° N. Many of them traveled eastwards for the first one or two days before entering the Arctic region. In cluster 6, trajectories started within a wide area of Siberia and extended also deeply into the continent (about 50° N in latitude). Such long-range transport is frequently found in winter for close to 18% of the time. Transport from Eastern Siberia with rare exceptions from Bering Sea and Alaska is presented by cluster 4 (10%) in Fig. 2a.

Compared to the atmospheric transport patterns in January, the cyclonic feature is much weaker and the length of trajectories is shorter in April, due to shifted and weakened surface pressure systems: the Siberian High, the Icelandic Low, and the Aleutian

Low (Serreze and Barry, 2005). Thus, long-range transport from the mid-latitudes is less frequent in spring compared to winter. The monthly average trajectory length in April is about 38% shorter than January between 1990 and 2005. In Fig. 2b, clusters 1 and 2 represent transport originated from the central and the northwestern North America, respectively. Cluster 3 is composed of trajectories from Eastern Siberia, and clusters 4 and 5 point to the Central Northern Siberia. Transport of air mass from Europe in April is only found in cluster 7.

According to the direction of each identified transport pathway, the linkage between the source of emission and the receptor is established. Tables 1 and 2 present the year-to-year changes in atmospheric transport frequency between 1990 and 2005 for winter and spring, respectively. In the North American sector, the frequency of atmospheric transport increases by about 10% from winter to spring. In the former USSR sector, transport from the Western and the Central USSR increases by 6% in spring compared to the winter pattern. Compared to that in winter, the frequency of transport from Europe in spring also decreases significantly by 15%.

3.2 Inter-annual variations of BC at Alert explained by the model

The transport frequency obtained in the previous section is then used here as f values in Eq. (2). Given monthly average BC measurements ([BC]), transport frequency (**f**), and surface BC flux (**E**), the linear regression model (Eq. 2) is solved using the least squares method, and the region specific b factors, as well as the individual p-values, are given in Table 3 for both seasons. The regressions are significant at 95% confidence level for both seasons. The time-series and the correlation between model reconstructed and the observed monthly average BC are shown in Fig. 3. Strong positive correlations are found between the model reconstructed and the observed BC at Alert for both seasons. The square of Pearson's correlation coefficient (R^2) indicates the inter-annual variations in observations explained by our linear regression model. As shown in Fig. 3, our model is able to explain 77% of the variation in the observed BC for winter, and over 80% is explained for spring, which is considerably better than

the approach in (Gong et al., 2010). Given the same BC emission dataset used in both studies, the better correlations obtained in this study are probably due to the implementation of 3-D trajectories followed by cluster analysis to better represent transport pathways affecting Alert rather than the pressure difference on a specific pressure level. It may also be partially due to the introduction of the pathway specific b factors, which implicitly account for the effect of atmospheric BC removal. Inter-annual variations can be considerably explained by this model which implies that atmospheric transport plays the dominant role in connecting source regions and the Canadian high Arctic site during the Arctic haze season. In such extreme cold season, favorable meteorological conditions, such as stable stratification, surface temperature inversion, and extreme dryness, suppress mixing, dry deposition, and wet scavenging of BC in the air and, therefore, enhance the long-range atmospheric transport.

About 20% of the inter-annual variation in observations cannot be explained by this approach. The uncertainty of this approach is affected by several assumptions made in the current study. First, the atmospheric removal mechanisms are not explicitly included in our approach. By assuming constant *b* factors with respect to the identified transport pathways, constant removal efficiencies during transport are implicitly assumed between 1990 and 2005. This assumption may not perfectly hold for years with extreme precipitation events. In January, 1997, for instance, the area averaged precipitation accumulation at the European sector is found the lowest among the period of interest, and it is estimated 33% lower than the multi-year average based on the Climate Prediction Center (CPC) Merged Analysis of Precipitation (CMAP) dataset (Huffman et al., 1997). Thus, the significant underestimation (about 25 ng/m^3 lower than the observation) in January, 1997 may be partly due to the extreme dry conditions, which substantially suppressed the wet scavenging of aerosols. In January 1995, however, the highest precipitation accumulation at the European sector (33% higher than the multi-year average) was found, which may partly explain the overestimation by our model. Another major source of uncertainty is the assumption that BC particles are uniformly distributed at the regions of emission. The BC emission inten-

sities used in this study does not consider the geographic distribution of BC within the potential source regions. Uncertainties of this approach may also come from trajectory calculation, emission data, and the implicit treatment of particle dry deposition and air mass mixing during the transport. To reduce all these sources of uncertainties, a study implementing the state-of-the-art aerosol model is on-going.

3.3 Source contributions to BC at Alert

According to the model, the contributions of BC transport from the North American and the Eurasia sectors are estimated based on the average of January and April from 1990 through 2005, as shown in Fig. 4. The annual BC emission intensities of North America and Eurasia are also shown for comparison. Comparing the importance of these two regions in affecting Alert, contributions from Eurasia dominate throughout the 16-year period. The model suggests that the Eurasia emitted BC contributes about 90 ng/m^3 (or 85%) to the measured BC particles at Alert, while the North America contributes less than 15 ng/m^3 (or 15%) on 16-year average. It agrees well with the most recent multi-model estimation (North America: 10% and Eurasia: 90%) (Shindell et al., 2008), considering the effects of South and East Asian emissions are not considered in this study. In January, the effect of the Eurasian emission becomes even more predominant (94%) than that in April (70%), which is due to the enhanced long-range transport in January. The results also agree with the case study conducted by Worth et al. (1994), for example, which attributed the observed peaks in BC concentration at Alert to long-range transport events from the Eurasian sector.

The model also suggests that the contribution of Eurasia declined significantly in the first 8–10 years since 1990. However, a slightly increasing trend can be noticed since the late 1990s to 2005 on the Eurasian contribution curve in Fig. 4. The relative importance of atmospheric transport and BC emission in governing the inter-annual variations of regional contributions to the near-surface BC level at Alert is also investigated. The Pearson's correlation coefficient between the Eurasian contribution and BC emission intensity from that region is found to be 0.93, which indicates that the inter-

annual change in Eurasian contributions is mainly attributed to regional BC emission reduction during the 16-year period rather than the changes in atmospheric transport. On the other hand, the correlation for the North American side is very poor ($R = 0.23$). So on the North American side, source contribution to BC levels at Alert for the same period did not simply depend on regional BC emission, but also on other factors, especially atmospheric transport patterns.

4 Conclusions

Based on the atmospheric transport frequency and the estimated BC emission intensity from surrounding regions, a linear regression model is constructed to investigate the inter-annual variations of BC observed at Alert in January and April, representative of winter and spring respectively, from 1990 through 2005. The atmospheric transport frequency is obtained by conducting cluster analysis on 10-day backward trajectories arriving at Alert. Annual BC emission intensity from potential source regions (i.e. European Union, former USSR, and North America) used in this study is an extended database initially developed by (Cooke et al., 1999). Solving the linear model, strong correlations are found between BC concentrations predicted with the regression model and measured at Alert for both seasons. The linear model is able to explain 77% of the inter-annual variation of BC for winter, and over 80% is explained for spring. Results imply that atmospheric transport and BC emission are the major contributors to the inter-annual variations in BC concentrations observed at Alert in the cold seasons for the 16-year period.

Based on the regression model the relative contributions of regional BC emissions affecting Alert are attributed to Eurasia and North America. Considering both seasons, the model suggests that Eurasia is the major contributor to the near-surface BC levels at the Canadian high Arctic site with an average contribution of over 85% during the 16-year period. In winter, the atmospheric transport of BC aerosols from Eurasia is found to be even more predominant with a multi-year average of 94%. The model esti-

ACPD
10, 2221–2244, 2010

mates smaller contribution from the Eurasian sector in spring (70%) than that in winter. Results suggest that atmospheric transport and BC emission played different roles in governing the inter-annual variations of regional contributions to the near-surface BC level at Alert. It is found that the change in Eurasian contributions depends mainly on the reduction of emission intensity. On the other hand, the inter-annual variation of the North American contributions was due to the changes in both emission and atmospheric transport. In agreement with (Gong et al., 2010), BC emission control in Eurasia seems to be an effective way to reduce BC levels in the Arctic lower troposphere.

Acknowledgements. The authors gratefully acknowledge the NOAA Air Resources Laboratory (ARL) for the provision of the HYSPLIT transport and dispersion model and READY website (http://www.arl.noaa.gov/ready.html) used in this publication.

References

Barrie, L. A.: Arctic air-pollution – an overview of current knowledge, Atmos. Environ., 20, 643–663, 1986.

Bond, T. C., Bhardwaj, E., Dong, R., Jogani, R., Jung, S., Roden, C., Streets, D. G., and Trautmann, N. M.: Historical emissions of black and organic carbon aerosol from energy-related combustion, 1850–2000, Global Biogeochem. Cy., 21, GB2018, doi:10.1029/2006GB002840, 2007.

Chung, C. E., V. Ramanathan, D. Kim, and I. A. Podgorny: Global anthropogenic aerosol direct forcing derived from satellite and ground-based observations, J. Geophys. Res.-Atmos., 110(17), D24207, doi:10.1029/2005JD006356, 2005.

Clarke, A. D. and Noone, K. J.: Soot in the Arctic snowpack – a cause for perturbations in radiative-transfer. Atmos. Environ., 19, 2045–2053, 1985.

Cooke, W. F., Liousse, C., Cachier, H., and Feichter, J.: Construction of a 1 degrees x 1 degrees fossil fuel emission data set for carbonaceous aerosol and implementation and radiative impact in the ECHAM4 model, J. Geophys. Res.-Atmos., 104, 22137–22162, 1999.

Dorling, S. R., Davies, T. D., and Pierce, C. E.: Cluster-analysis – a technique for estimating

the synoptic meteorological controls on air and precipitation chemistry – method and applications, Atmos. Environ., 26, 2575–2581, 1992.
Eckhardt, S., Stohl, A., Beirle, S., Spichtinger, N., James, P., Forster, C., Junker, C., Wagner, T., Platt, U., and Jennings, S. G.: The North Atlantic Oscillation controls air pollution transport to the Arctic, Atmos. Chem. Phys., 3, 1769–1778, 2003, http://www.atmos-chem-phys.net/3/1769/2003/.
Flanner, M. G., Zender, C. S., Randerson, J. T., and Rasch, P. J.: Present-day climate forcing and response from black carbon in snow, J. Geophys. Res.-Atmos., 112(17), D11202, doi:10.1029/2006JD008003, 2007.
Gong, S. L., Zhao, T. L., Sharma, S., Toom-Sauntry, D., Lavoue, D., Zhang, X. B., Leaitch, W. R., and Barrie, L.: Identification of trends and inter-annual variability of sulphate and black carbon in the Canadian High Arctic: 1981 to 2007, J. Geophys. Res.-Atmos., available online at: http://www.agu.org/journals/pip/jd/2009JD012943-pip.pdf, doi:10.1029/2009JD012943, in press, 2010.
Hansen, J. and L. Nazarenko: Soot climate forcing via snow and ice albedos. Proc. Natl. Acad. Sci. USA, 101, 423–428, 2004.
Harris, J. M. and Kahl, J. D.: A Descriptive Atmospheric Transport Climatology for the Mauna-Loa-Observatory, Using Clustered Trajectories, J. Geophys. Res.-Atmos., 95, 13651–13667, 1990.
Harris, J. M. and Kahl, J. D. W.: Analysis of 10-Day Isentropic Flow Patterns for Barrow, Alaska – 1985–1992, J. Geophys. Res.-Atmos., 99, 25845–25855, 1994.
Huffman, G. J., Adler, R. F., Arkin, P., Chang, A., Ferraro, R., Gruber, A., Janowiak, J., McNab, A., Rudolf, B., and Schneider, U.: The Global Precipitation Climatology Project (GPCP) Combined Precipitation Dataset, B. Am. Meteorol. Soc., 78, 5–20, 1997.
Jacobson, M. Z.: Strong radiative heating due to the mixing state of black carbon in atmospheric aerosols, Nature, 409, 695–697, 2001.
Jacobson, M. Z.: Climate response of fossil fuel and biofuel soot, accounting for soot's feedback to snow and sea ice albedo and emissivity, J. Geophys. Res.-Atmos., 109(15), D21201, doi:10.1029/2004JD004945, 2004.
Kahl, J. D.: Characteristics of the Low-Level Temperature Inversion Along the Alaskan Arctic Coast, Int. J. Climatol., 10, 537–548, 1990.
Kalnay, E., Kanamitsu, M., Kistler, R., Collins, W., Deaven, D., Gandin, L., Iredell, M., Saha, S., White, G., Woollen, J., Zhu, Y., Chelliah, M., Ebisuzaki, W., Higgins, W., Janowiak, J., Mo,

K. C., Ropelewski, C., Wang, J., Leetmaa, A., Reynolds, R., Jenne, R., and Joseph, D.: The NCEP/NCAR 40-year reanalysis project, B. Am. Meteorol. Soc., 77, 437–471, 1996.
Kim, Y., Hatsushika, H., Muskett, R. R., and Yamazaki, K.: Possible effect of boreal wildfire soot on Arctic sea ice and Alaska glaciers, Atmos. Environ., 39, 3513–3520, 2005.
Koch, D. and Hansen, J.: Distant origins of Arctic black carbon: A Goddard Institute for Space Studies ModelE experiment, J. Geophys. Res.-Atmos., 110(14), D04204, doi:10.1029/2004JD005296,, 2005.
Kristjansson, J. E., Iversen, T., Kirkevag, A., Seland, O., and Debernard, J.: Response of the climate system to aerosol direct and indirect forcing: Role of cloud feedbacks, J. Geophys. Res.-Atmos., 110(13), D24206, doi:10.1029/2005JD006299, 2005.
Law, K. S. and Stohl, A.: Arctic air pollution: Origins and impacts, Science, 315, 1537–1540, 2007.
Lin, C. J., Cheng, M. D., and Schroeder, W. H.: Transport patterns and potential sources of total gaseous mercury measured in Canadian high Arctic in 1995, Atmos. Environ., 35, 1141–1154, 2001.
Quinn, P. K., Shaw, G., Andrews, E., Dutton, E. G., Ruoho-Airola, T., and Gong, S. L.: Arctic haze: current trends and knowledge gaps, Tellus B-Chem. Phys. Meteorol., 59, 99–114, 2007.
Ramanathan, V. and Carmichael, G.: Global and regional climate changes due to black carbon, Nature Geoscience, 1, 221–227, 2008.
Serreze, M. C. and Barry, R. G.: The Arctic Climate System, Cambridge University Press, 385 pp., 2005.
Sharma, S., Lavoue, D., Cachier, H., Barrie, L. A., and Gong, S. L.: Long-term trends of the black carbon concentrations in the Canadian Arctic, J. Geophys. Res.-Atmos., 109(10), D15203, doi:10.1029/2003JD004331, , 2004.
Sharma, S., Andrews, E., Barrie, L. A., Ogren, J. A., and Lavoue, D.: Variations and sources of the equivalent black carbon in the high Arctic revealed by long-term observations at Alert and Barrow: 1989–2003, J. Geophys. Res.-Atmos., 111(15), D14208, doi:10.1029/2005JD006581,, 2006.
Sharma, S., Ishizawa, M., Chan, D., Lavoué, D., Leaitch, R., Worthy, D., Andrews, E., Eleftheriadis, K., Mefford, T., and Maksyutov, S.: Synoptic Transport of Anthropogenic BC to the Arctic, NOAA annual conference, Boulder, CO, USA, 2009.
Shaw, G. E.: The arctic haze phenomenon., B. Am. Meteorol. Soc., 76, 2403–2413, 1995.

Shindell, D. T., Chin, M., Dentener, F., Doherty, R. M., Faluvegi, G., Fiore, A. M., Hess, P., Koch, D. M., MacKenzie, I. A., Sanderson, M. G., Schultz, M. G., Schulz, M., Stevenson, D. S., Teich, H., Textor, C., Wild, O., Bergmann, D. J., Bey, I., Bian, H., Cuvelier, C., Duncan, B. N., Folberth, G., Horowitz, L. W., Jonson, J., Kaminski, J. W., Marmer, E., Park, R., Pringle, K. J., Schroeder, S., Szopa, S., Takemura, T., Zeng, G., Keating, T. J., and Zuber, A.: A multi-model assessment of pollution transport to the Arctic, Atmos. Chem. Phys., 8, 5353–5372, 2008, http://www.atmos-chem-phys.net/8/5353/2008/.

Stohl, A.: Characteristics of atmospheric transport into the Arctic troposphere, J. Geophys. Res.-Atmos., 111(17), D11306, doi:10.1029/2005JD006888, 2006.

United Nations: The United Nations energy statistics database (2005), 5 pp., 2007.

Worthy, D. E. J., Trivett, N. B. A., Hopper, J. F., Bottenheim, J. W., and Levin, I.: Analysis of Long-Range Transport Events at Alert, Northwest-Territories, During the Polar Sunrise Experiment, J. Geophys. Res.-Atmos., 99, 25329–25344, 1994.

Table 1. Inter-annual variation of transport frequency (trajectory number of each sector divided by the total number of trajectories, in percentage) affecting Alert in January, 1990–2005.

	North America	Former USSR				European Union	
	Cluster 2	Cluster 3	Cluster 4	Cluster 5	Cluster 6	Cluster 1	Cluster 7
1990	25%	3%	0%	0%	17%	33%	21%
1991	55%	0%	7%	10%	17%	9%	2%
1992	30%	4%	10%	32%	6%	11%	8%
1993	14%	42%	3%	0%	27%	14%	0%
1994	5%	2%	19%	19%	33%	11%	12%
1995	12%	4%	6%	37%	25%	13%	3%
1996	31%	26%	11%	4%	9%	18%	0%
1997	11%	6%	9%	10%	21%	1%	43%
1998	19%	5%	18%	7%	11%	31%	10%
1999	1%	15%	2%	8%	0%	70%	4%
2000	43%	29%	6%	10%	7%	6%	0%
2001	26%	13%	0%	14%	20%	15%	11%
2002	2%	3%	16%	14%	39%	10%	15%
2003	15%	21%	18%	19%	7%	15%	3%
2004	23%	5%	28%	4%	34%	2%	2%
2005	18%	6%	1%	21%	9%	19%	27%
Average	21%	52%				27%	

ACPD
10, 2221–2244, 2010

Table 2. Same as Table 1, but for April, 1990–2005.

	North America		Former USSR				European Union
	Cluster 1	Cluster 2	Cluster 3	Cluster 4	Cluster 5	Cluster 6	Cluster 7
1990	15%	11%	38%	13%	2%	0%	22%
1991	1%	16%	26%	16%	0%	41%	1%
1992	38%	0%	13%	2%	20%	17%	11%
1993	2%	4%	24%	40%	12%	8%	9%
1994	33%	8%	21%	4%	19%	5%	11%
1995	19%	7%	16%	16%	27%	0%	15%
1996	19%	0%	6%	0%	0%	0%	74%
1997	22%	4%	8%	4%	11%	38%	14%
1998	8%	17%	6%	0%	9%	43%	17%
1999	11%	12%	21%	8%	40%	8%	0%
2000	39%	11%	29%	14%	5%	2%	0%
2001	37%	4%	18%	38%	1%	1%	0%
2002	0%	69%	14%	10%	0%	7%	0%
2003	3%	5%	52%	15%	7%	17%	1%
2004	25%	11%	7%	15%	22%	8%	13%
2005	36%	1%	26%	12%	19%	6%	0%
Average	30%		58%				12%

ACPD
10, 2221–2244, 2010

Table 3. Values of b_i factors for January and April, 1990–2005.

	b_1	b_2	b_3	b_4	b_5	b_6	b_7
January	11.0	68.4	100.3	192.7	167.1	181.4	43.7
p-value	0.048	0.081	0.088	0.082	0.017	0.006	0.006
April	65.8	54.8	137.6	113.8	129.0	62.6	9.2
p-value	0.037	0.045	0.002	0.046	0.045	0.046	0.048

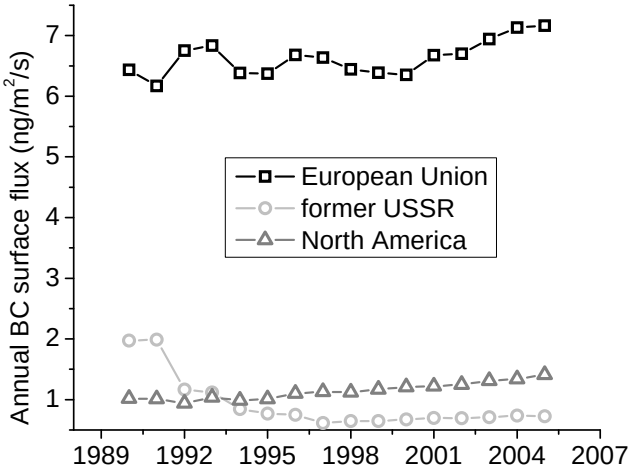

Fig. 1. Annual average BC surface flux (ng/m^2/s) from European Union, the former USSR, and North America: 1990–2005.

ACPD
10, 2221–2244, 2010

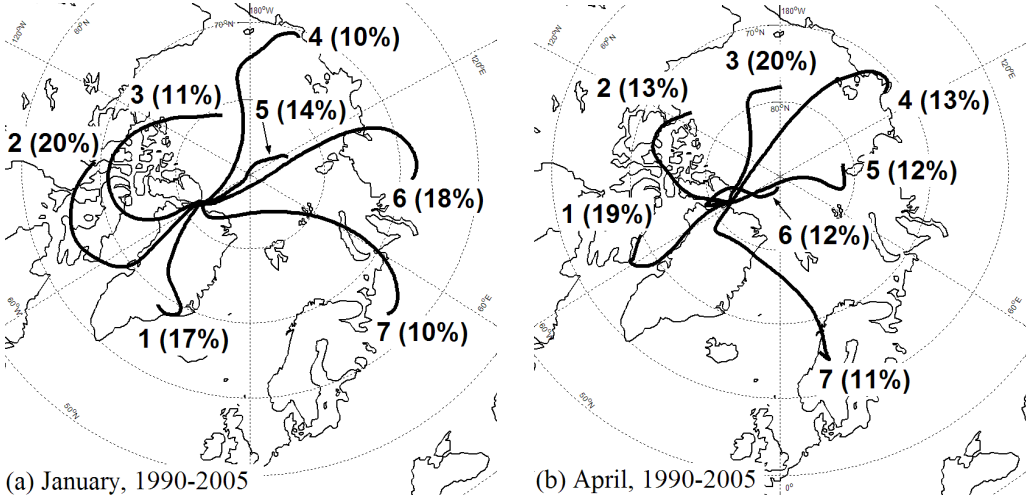

Fig. 2. Transport pathways affecting Alert, Nunavut in January **(a)** and April **(b)** from 1990 through 2005 identified by cluster analysis on the HYSPLIT trajectories. The number outside the brackets serves only as an identification of each cluster; the one inside the brackets gives the frequency of occurrence of the underlining transport pathway.

ACPD
10, 2221–2244, 2010

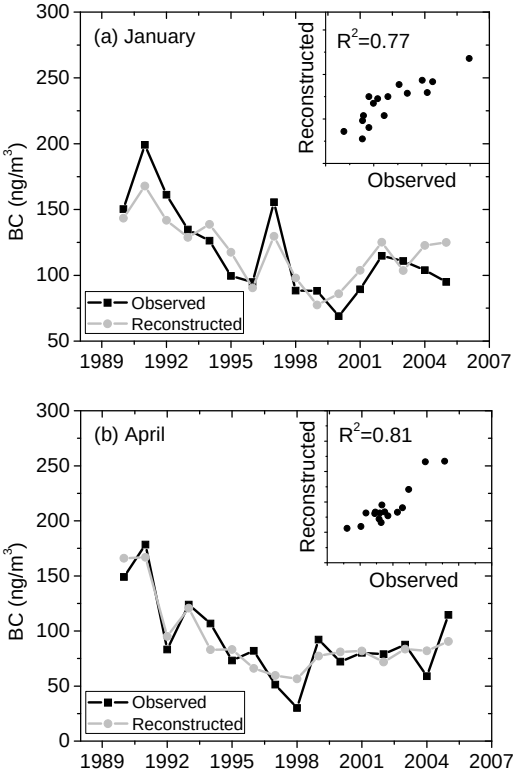

Fig. 3. Time-series of the model reconstructed and the observed monthly average BC in January **(a)** and April **(b)**, 1990–2005. The R^2 shown in both plots are the squires of the Pearson's correlation coefficients between the reconstructed and observed BC concentrations rather than those for linear regressions.

ACPD
10, 2221–2244, 2010

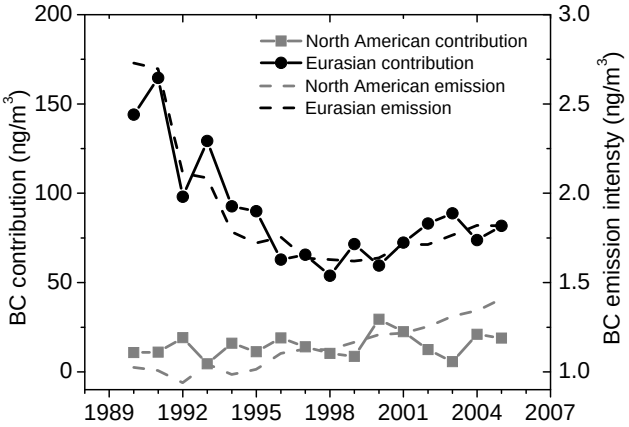

Fig. 4. Model estimated source contributions of BC from the North American and the Eurasian sectors based on the average of January and April from 1990 through 2005. The inter-annual changes in BC emission intensity are show by two dashed lines.

ACPD
10, 2221–2244, 2010